

RESEARCH PAPER

 OPEN ACCESS



Influence of the loop size and nucleotide composition on AgoshRNA biogenesis and activity

Elena Herrera-Carrillo, Alex Harwig, and Ben Berkhout

Laboratory of Experimental Virology, Department of Medical Microbiology, Center for Infection and Immunity Amsterdam (CINIMA), Academic Medical Center, University of Amsterdam, AZ Amsterdam, the Netherlands

ABSTRACT

Short hairpin RNAs (shRNAs) are widely used for gene silencing by the RNA interference (RNAi) mechanism. The shRNA precursor is processed by the Dicer enzyme into active small interfering RNAs (siRNAs) that subsequently target a complementary mRNA for cleavage by the Argonaute 2 (Ago2) complex. Recent evidence indicates that shRNAs with a relatively short basepaired stem bypass Dicer and are instead processed by Ago2. We termed these molecules AgoshRNAs as both processing and silencing steps are mediated by Ago2 and proposed rules for the design of effective AgoshRNA molecules. Active and non-cytotoxic AgoshRNAs against HIV-1 RNA were generated, but their silencing activity was generally reduced compared with the matching shRNAs. Thus, further optimization of the AgoshRNA design is needed. In this study, we evaluated the importance of the single-stranded loop, in particular its size and nucleotide sequence, in AgoshRNA-mediated silencing. We document that the pyrimidine/purine content is important for AgoshRNA-mediated silencing activity.

ARTICLE HISTORY

Received 13 January 2017
Revised 4 May 2017
Accepted 5 May 2017

KEYWORDS

Ago2; Dicer; Dicer-independent shRNA; HIV-1; miR-451; RNAi; shRNA design



Introduction


RNAi is a cellular mechanism that uses micro RNA (miRNA) molecules to regulate gene expression at the post-transcriptional level.^{1–4} Man-made shRNAs can be used to induce post-transcriptional gene silencing. Similar to miRNAs, shRNAs are transcribed in the nucleus, transported to the cytoplasm by Exportin-5 and processed by Dicer into the active siRNA duplex. The siRNA associates with Ago2 to form the RNA-induced silencing complex (RISC) that induces degradation of complementary target mRNAs.^{5–7} Thermodynamic properties of the RNA duplex determine which strand will be selected as guide by RISC.^{8,9} The passenger strand of the duplex is degraded.

Alternatively, RISC can also accommodate certain pre-miRNAs in the absence of Dicer. More specifically, miR-451 with a short 18 base pair (bp) stem and 4 nt loop (AGUU) is instead processed by Ago2. Ago2 cleaves the duplex on the 3' side between bp 10 and 11, thus generating a single extended 30 nt guide strand that is further trimmed by poly(A)-specific ribonuclease (PARN) to create the ~22–26 nt mature miR-451.^{10–13} Recent studies indicated that short shRNAs which mimic miR-451 are also processed by Ago2 instead of Dicer.^{14–18} We called these AgoshRNA molecules, as both the processing and silencing function are mediated by Ago2. These alternative processing routes are depicted in Fig. 1A. Regular shRNAs are processed by Dicer (left panel), but AgoshRNA (≤ 18 bp)

avoid Dicer recognition and are instead processed by Ago2 (right panel). Dicer generates the duplex siRNA with candidate guide and passenger strands (left panel, marked black-3' and white-5', respectively). AgoshRNA molecules are loaded and cleaved by Ago2 that generates a single guide strand which - upon PARN processing - yields the Agosh^{TRIM} molecule, which is the most abundant form in Ago2 complexes.¹⁶ These 3 AgoshRNA forms are shown in gray in the right panel of Fig. 1A. The novel AgoshRNA design has the clear advantage over regular shRNAs of not producing a passenger strand that may cause off-target effects. The use of shorter AgoshRNA hairpins in therapeutic applications seems beneficial because innate immunity sensors like interferon will be triggered less efficiently.¹⁹ We previously listed other advantages of AgoshRNA inhibitors, including the ability to remain active in Dicer-minus cells such as monocytes.²⁰

We converted a set of potent anti-HIV-1 shRNAs into AgoshRNAs by shifting the guide sequence from the 3' to the 5'-side of a shortened hairpin, but this manipulation affected the gene silencing efficacy.²¹ We therefore tried to optimize the AgoshRNA design. First, we tested whether a weak G-U bp at the top of the hairpin stem is advantageous for Ago2 processing. Optimization was described for several AgoshRNAs, but the effect was not general.¹⁴ Second, we documented the importance of the 5-terminal nt identity and its basepairing status for AgoshRNA activity. AgoshRNA activity is enhanced by

CONTACT Ben Berkhout  b.berkhout@amc.uva.nl  Laboratory of Experimental Virology, Department of Medical Microbiology, Center for Infection and Immunity Amsterdam (CINIMA), Academic Medical Center, University of Amsterdam, Meibergdreef 15, 1105 AZ Amsterdam, the Netherlands.

 Supplemental data for this article can be accessed on the [publisher's website](#).

© 2017 Elena Herrera-Carrillo, Alex Harwig, and Ben Berkhout. Published with license by Taylor & Francis Group, LLC

This is an Open Access article distributed under the terms of the Creative Commons Attribution-NonCommercial License (<http://creativecommons.org/licenses/by-nc/4.0/>), which permits unrestricted non-commercial use, distribution, and reproduction in any medium, provided the original work is properly cited. The moral rights of the named author(s) have been asserted.

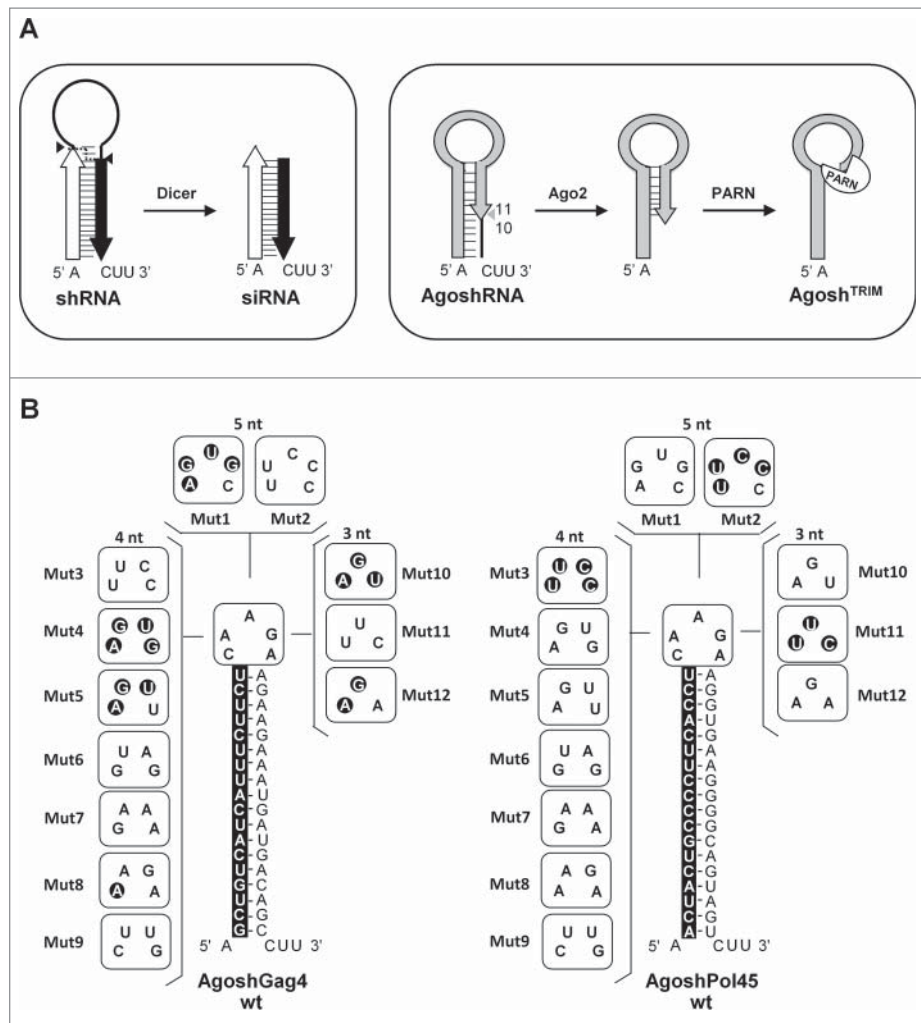


Figure 1. Design of anti-HIV AgoshRNA mutants varying in loop size and nucleotide composition. (A) In the canonical pathway (left) the shRNA stem is cleaved by Dicer into a siRNA duplex of ~21 bp with 3' UU overhang that is loaded into RISC. The 5' passenger (white arrow) is cleaved and degraded and the 3' guide strand (black arrow) acts in RNAi-silencing. In the non-canonical pathway (right), the AgoshRNA is cleaved by Ago2 on the 3' side between bp 10 and 11 into an extended guide of ~30 nt (gray arrow). AgoshRNA is trimmed by PARN to create a ~24 nt guide named Agosh^{TRIM} and subsequently may instruct Ago2 for RNAi-silencing. The predicted Dicer and Ago2 cleavage sites are marked with black and gray arrows, respectively. (B) Secondary structure of the Gag4 and Pol45 AgoshRNA molecules with the guide strand boxed in black. The 5' end nt of AgoshRNA constructs and its basepairing partner were replaced by A C. The terminal loop was mutated into 12 loop variants differing in loop size (3–5 nt) and sequence. We grouped them according to loop size: 3 nt on the right, 4 nt on the left and 5 nt on top.

introduction of a bottom mismatch and 5'-terminal A or G.²² These small RNAs are usually synthesized by the H1 polymerase III promoter, which requires a purine at the +1 position for optimal transcriptional efficiency. We selected A over G because the MID domain of the human Ago2 protein prefers to load small RNAs with U or A as 5'-end.^{23,24} Third, we tested whether the introduction of weak G-U/U-G bp along the AgoshRNA stem, without affecting the guide sequence, could boost the silencing activity. However, G-U introduction rather destroyed the AgoshRNA activity.²¹ These combined results allowed us to propose general rules for the design of AgoshRNA molecules with significantly improved silencing activity and potent, non-cytotoxic anti-HIV-1 AgoshRNA molecules were generated (Herrera et al., ref. 49). However, the AgoshRNA silencing activity was reduced compared with that of the matching shRNAs. Therefore, further optimization of the AgoshRNA design is warranted.

The loop sequence and structure influences the activity of regular shRNAs, in part through an effect on Dicer

recognition and processing.^{17,25} Mutation of the loop sequence can also affect or even abrogate miRNA processing.^{26,27} We wondered whether the loop size or sequence affects the activity of AgoshRNA molecules. We previously observed that large loops (> 7 nt) cause a partial return from Ago2 to regular Dicer processing, possibly by steric hindrance during Ago2 binding.²⁸ The loop sequence may also influence the subsequent silencing step because the loop is part of the extended AgoshRNA guide strand (Fig. 1A, right panel). In this study, we analyzed how AgoshRNA activity is influenced by systematic mutation of the small 3–5 nt loop to establish new design rules.

Results

AgoshRNA design

We tested the effect of different loop sequences, varying in size and composition, on AgoshRNA-mediated gene silencing (Fig. 1B). Two candidate anti-HIV-1 AgoshRNA molecules

were selected as substrates for the current mutational analysis (AgoshGag4 and AgoshPol45). All tested AgoshRNA mutants have a duplex length of 18 bp and a bottom A C mismatch, but we varied the sequence of the single-stranded loop. The encoded anti-HIV-1 guide sequence on the 5' side of the duplex is highlighted in black. The 12 mutants differ in loop size (3–5 nt) and are grouped accordingly in Fig. 1B (5 nt: Mut1 and 2, 4 nt: Mut3–9, 3 nt: Mut10–12). The same set of 12 loop mutants was constructed for both substrates (AgoshGag4 and AgoshPol45). RNA structure prediction algorithms indicated only minimal effects on the thermodynamic stability of the hairpins (< 0.6 kcal/mol difference), except for significant stabilization of Mut7 (-2.7 kcal/mol) and Mut9 (-1.0 kcal/mol) for both AgoshGag4 and AgoshPol45. This survey includes a test of whether extension of the mRNA-complementarity of the guide strand over the loop can boost the AgoshRNA activity (nt highlighted in black for AgoshGag4: Mut1, 4 and 10; AgoshPol45: Mut2, 3 and 11). We also inserted the miR-451 loop (Mut5), which may have been optimized during evolution for Ago2-mediated processing and silencing activity.²⁹ We also included the particularly stable CUUG tetraloop (Mut9) in which the first and fourth nt form a Watson and Crick bp that makes this tetraloop resistant to degradation.³⁰ Other commonly used tetra and triloops were also tested (Mut6–8 and 12).^{17,18,31}

Silencing activity of the AgoshRNAs loop mutants

To evaluate the inhibitory activity of the designed AgoshRNA molecules, we co-transfected HEK293T cells with the H1-driven AgoshRNA construct and a luciferase reporter with the sense HIV-target sequence (Luc-sense) or a control reporter encoding the antisense HIV-1 sequence (Luc-antisense) (Fig. 2A). We titrated the AgoshRNA construct (1, 5 and 25 ng). The Luc-sense reporter detects the activity of the shRNA 5'-passenger strand (white arrow) and the extended 5'-guide strand of AgoshRNAs (gray arrow). Luc-antisense will score shRNA 3'-guide strand activity (black arrow). The 3'-end leftover of processed AgoshRNA (~ 10 nt) is not expected to be active. A fixed amount of renilla luciferase plasmid was included to control for the transfection efficiency. Firefly and renilla luciferase was measured in cellular lysates made 2 d post-transfection and the ratio was used to calculate the relative luciferase activity (Figs. S1 and S2). The Luc-activity measured in the presence of the unrelated shNef construct was set at 100%. A clear dose-dependent knockdown activity was measured for all AgoshRNA mutants on the Luc-sense reporter and no activity was apparent on the Luc-antisense reporter. Fig. 2B and C show the results obtained with a sub-optimal AgoshRNA concentration (5 ng), thus within the linear range of the assay. We will first describe the results obtained for the AgoshGag4 set and subsequently the AgoshPol45 mutants.

AgoshGag4 wild-type (wt) showed good inhibitory activity on the Luc-sense reporter, with luciferase levels dropping to approximately 15% of the uninhibited value, and exercised no activity on the Luc-antisense reporter (Fig. 2B). The loop mutants exhibited variable silencing activity on the Luc-sense

reporter, with luciferase levels ranging from 10% to 40% of the uninhibited value, but all mutants showed very little or no activity on the Luc-antisense reporter. On the Luc-sense reporter, we compared the knockdown activity of AgoshRNA variants with 5 (Mut1 and 2), 4 (Mut3–9) and 3 (Mut10–12) nt loops and did not find a correlation between loop size and activity. For instance, mutants with a similar loop sequence but different loop size (e.g. Mut1, 4 and 10) demonstrated similar knockdown activity. Only Mut12 with a loop of only 3 nt (AGA) showed enhanced knockdown activity when compared with the wt, but not all triloops resulted in increased activity (Mut10 and 11). Thus, the loop size in the 3–5 nt range is not a critical determinant of AgoshRNA activity, but the loop sequence may contribute, possibly through a structural effect on AgoshRNA processing or activity.

We wondered whether we could boost AgoshRNA activity by making the loop more stable as previously suggested.^{18,32} We did not score improved, but rather profoundly reduced silencing activity with a particularly stable tetraloop (CUUG, Mut9). We also tested whether extension of the guide strand complementarity over the loop enhanced AgoshRNA activity, but measured no increased knockdown potency for Mut1, 4 and 10. We tried to optimize the AgoshRNA design by introduction of the miR-451 loop (Mut5), but wt activity was scored. Inspection of the data sets alerted us to the putative importance of the Purine (Pu)/Pyrimidine (Py) content of the loop. Strikingly, we observed that a high Py content correlated with impaired Luc-sense knockdown activity (e.g., Mut2, 3, 9 and 11), whereas a high Pu content correlated with good wt like-activity (Mut4, 7, 10 and 12).

General AgoshRNA loop improvements

It is important to determine whether the observed loop trends are of general value. To test if the findings also apply to other AgoshRNAs, we introduced the complete mutant loop set in the unrelated AgoshPol45 molecule, which exhibited sub-optimal anti-HIV-1 activity. The loop mutants exhibited variable, but modest silencing activities on the Luc-sense reporter, with luciferase levels ranging from 50% to only 90% of the uninhibited value, but the AgoshRNAs showed very little or no activity on the Luc-antisense reporter (Fig. 2C). Overall, the AgoshPol45 trends were similar to that observed for AgoshGag4, as illustrated in Fig. 3A. Most strikingly, the efficacy of AgoshPol45 improved when the wt loop was replaced by the triloop AGA (Mut12). Again, loops with a high Py content (Mut2, 3, 9 and 11) showed decreased silencing efficacy. Only Mut4 behaved differently in AgoshPol45 versus AgoshGag4 and resulted in a dramatic loss of AgoshPol45 activity only. Possibly, this could be the result of extended guide complementarity in AgoshGag4 (Fig. 1B). These combined results indicate that the activity of good and moderately active AgoshRNAs can be improved by varying the loop composition, but not dramatically.

To confirm the improved activity of the AGA triloop (Mut12), we next performed a titration by 2-fold serial dilutions in the 0.8 - 25 ng range. Firefly and renilla luciferase activity was measured in cellular lysates obtained at 2 d post-transfection and the ratio was used to calculate the relative

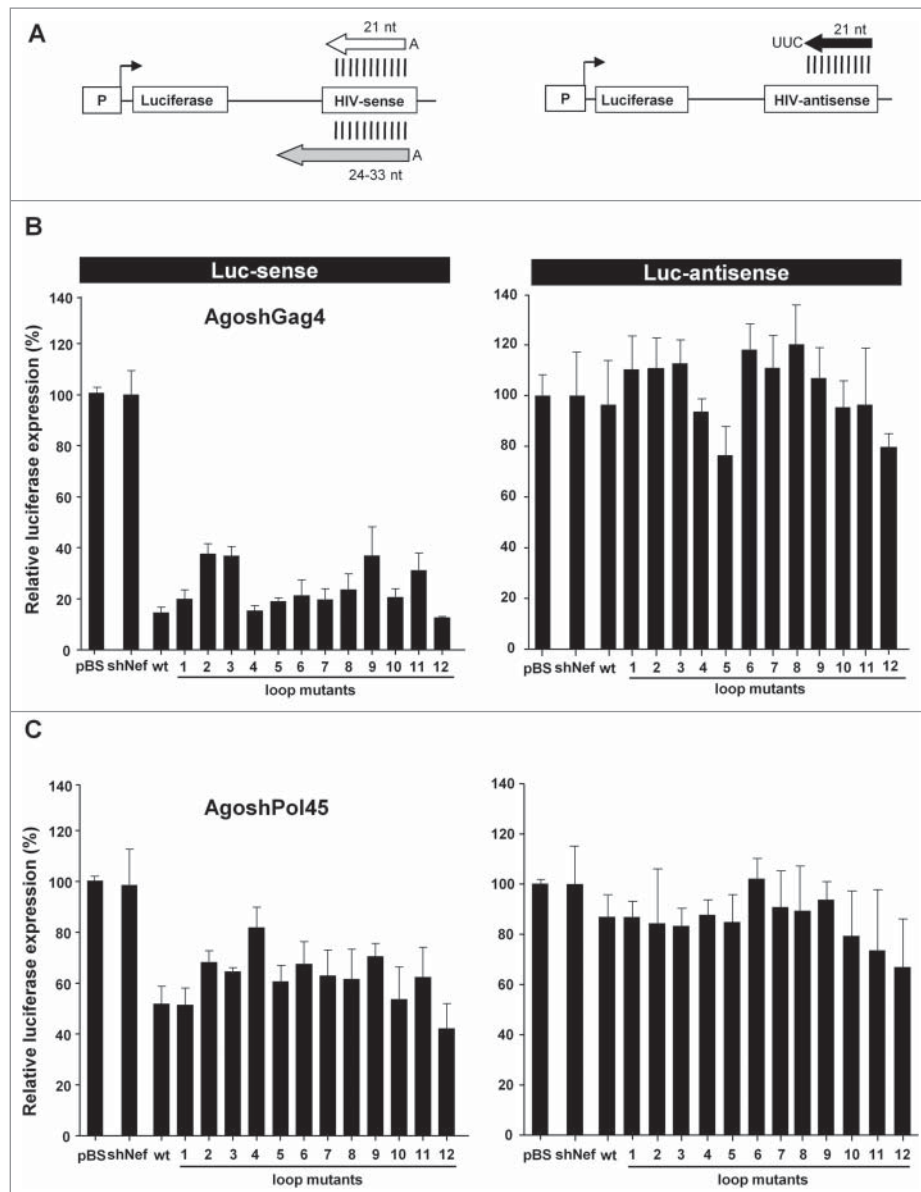


Figure 2. Luciferase knockdown activity of the AgoshRNA loop mutants. (A) Luciferase reporter constructs with a sense (left panel) or antisense (right panel) HIV-derived sequence are shown. The Luc-sense reporter scores canonical shRNA guide activity (white arrow) and AgoshRNA activity (gray extended arrow). The Luc-antisense reporter scores shRNA passenger activity (black arrow). Luciferase knockdown was determined by co-transfection of the reporters with (B) the AgoshGag4 or (C) the AgoshPol45 constructs. HEK293T cells were co-transfected with 100 ng of the respective firefly luciferase reporter plasmid, 1 ng of renilla luciferase plasmid, and 5 ng of the AgoshRNA constructs. An irrelevant shRNA (shNef) served as negative control, for which the activity was set at 100% luciferase expression. The mean values and standard deviation are based on 6 independent transfections.

luciferase activity (Fig. 3B). The activity measured in the presence of the unrelated shNef construct was set at 100%. A clear dose-dependent knockdown activity was measured, and Mut12 consistently outperformed wt for both AgoshRNA molecules. The effect was more pronounced for the moderately active AgoshPol45, especially at low AgoshRNA concentrations.

Antiviral activity of the AgoshRNA loop mutants

The complete sets of AgoshGag4 and AgoshPol45 mutants were tested for their ability to inhibit HIV-1 production. A sub-optimal amount of each AgoshRNA expression construct (5 ng) was co-transfected with the HIV-1 molecular clone pLAI (250 ng) in HEK293T cells. A fixed amount of

renilla luciferase plasmid was included to control for variation in transfection efficiency. Two days post-transfection, HIV-1 production was analyzed by measuring the viral capsid protein (CA-p24) level in the culture supernatant, which was corrected for the renilla luciferase activity (Fig. 4). Virus production in the presence of 5 ng control plasmid pBluescript (pBS) was set at 100%. Inhibition of HIV-1 production revealed similar results as the luciferase assays (Fig. 4 left and right panels, compare with Fig. 2B and C, respectively). For instance, antiviral activity of the wt AgoshGag4 and AgoshPol45 improved significantly when the loop was replaced by the triloop AGA (Mut12). Furthermore, AgoshRNA loops with a high Py content (Mut2, 3, 9 and 11) showed decreased silencing efficacy.

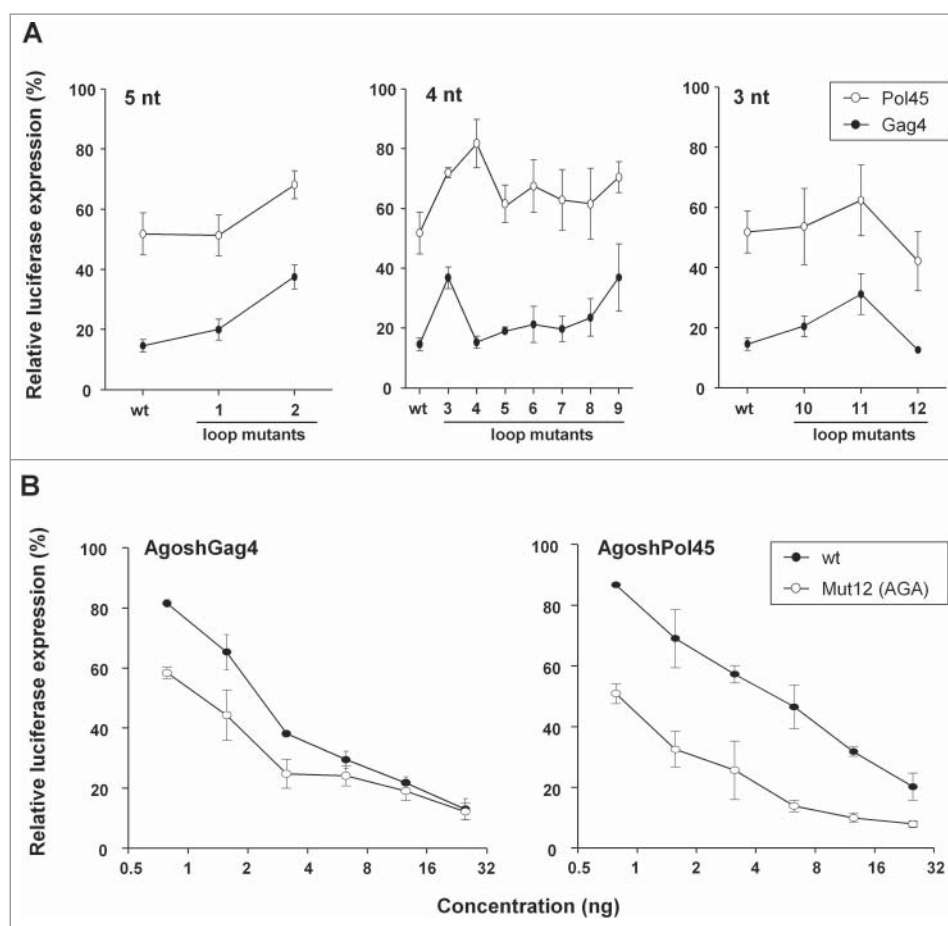


Figure 3. Influence of the loop sequence on AgoshRNA-mediated silencing. (A) Luciferase knockdown by wild-type (wt) and mutant versions of AgoshGag4 (black dots) and AgoshPol45 (white dots). Mutants were grouped according to the loop size in three panels. (B) Luciferase knockdown upon titration of the AgoshRNA constructs (2-fold serial dilutions, 0.8–25 ng). An irrelevant shRNA (shNef) served as negative control, for which the activity was set at 100% luciferase expression. The mean values and standard deviation are based on 6 independent transfections.

Processing of the AgoshRNA mutants

The range of silencing activities observed for different AgoshRNA loop mutants might reflect altered RNAi activity, but could also be due to differences in RNA processing by Ago2 or differences in intracellular stability. To investigate why specific loops make the AgoshRNA more or less effective in gene silencing, northern blot analysis was performed for all AgoshRNA variants (Fig. 5). The unrelated shNef was used as negative control. Processing of the 5'-guide and 3'-passenger strands of the AgoshRNAs was analyzed with a “guide” probe (top panels) and a “passenger” probe (bottom panels). We will first describe the results observed for the AgoshGag4 set (Fig. 5A). The “guide” probe detected 2 bands of ~30 and ~24 nt (top panel), which likely represent the extended guide strand and its 3'-trimmed product AgoshRNA^{TRIM}. This was confirmed by deep sequencing analysis of the transcripts, which also indicated that the loop mutations do not affect the end point of 3'-trimming (results not shown). As expected, we observed minor shifts in gel migration of the AgoshRNA signals due to differences in loop size (Mut1–2 > Mut3–9 > Mut11–13). In fact, only the larger ~30 nt RNA signal is weakly detected with the “passenger” probe (lower panel). Limited complementarity of the “passenger” probe to the processed RNA products may explain the reduced intensity of this signal and the absence of the trimmed product. As described previously, the 10 nt 3'-

terminal product of processed AgoshRNAs is not detected with the “passenger” probe, possibly because it is rapidly degraded.¹⁷ Importantly, no Dicer-processed products of ~21 nt were detected for the wt and mutant AgoshGag4 molecules, consistent with exclusive Ago2-mediated processing.

We observed differences in guide RNA abundance on the RNA gel blot that do not seem to correlate with the measured knockdown activity. For instance, Mut1 is more abundant than wt, thus possibly more stable, but nevertheless less active. Among the tetraloop mutants, Mut5 with the miR-451 loop is most abundant, but certainly not the most active. Mut10–12 also exhibit differences in RNA abundance that do not correlate with the measured knockdown activity. For instance, Mut10 is more abundant, but less active than Mut12.

Bands of ~24 and ~30 nt in length were also observed for the AgoshPol45 set (Fig. 5B, top panel), which represent the extended guide strand and the 3'-trimmed product. Again the 10 nt 3'-terminal product of processed AgoshRNAs is not detected with the “passenger” probe (lower panel). Regular Dicer products of ~21 nt were not detected for the wt and mutant AgoshPol45 molecules. In general, the abundance patterns were similar but not identical to that observed for the AgoshGag4 mutant set. Thus again, AgoshPol45 abundance was not always consistent with the measured knockdown

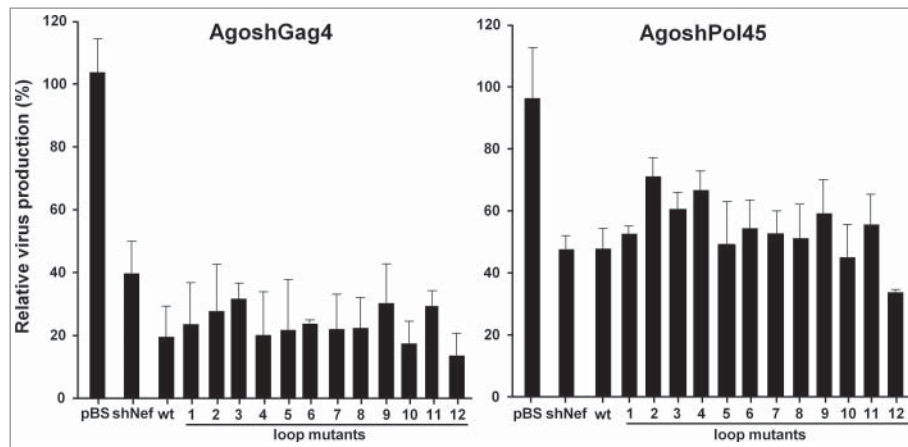


Figure 4. Inhibition of HIV-1 production by AgoshRNA loop mutants. HEK293T cells were co-transfected with 250 ng of the HIV-1 pLAI, 1 ng of renilla luciferase plasmid (pRL) and 25 ng of the AgoshRNA constructs. Two days post-transfection, inhibition of HIV-1 production was determined by measuring CA-p24 levels in the culture supernatant. CA-p24 values were normalized to the renilla luciferase activities. The ratio between the CA-p24 level and the renilla luciferase activity in the presence of 5 ng pBS control was set at 100%. Bars represent the average values from 8 independent transfections and error bars shows the standard deviation.

activity. Mut4 may form an exception as this mutant is less active, consistent with the greatly reduced abundance of the RNA signal. Strikingly, Mut5 with the miR-451 loop again produced the most abundant RNA signals, which might reflect enhanced RNA stability. However, increased RNA abundance did not result in enhanced knockdown activity. Products of ~21 nt that would be expected for alternative Dicer-processing were not detected, demonstrating the effective shRNA into AgoshRNA conversion. To summarize, variable activity was scored for the AgoshRNA

variants, but this did not frequently correlate with the amount of processed RNA present in cells. This would mean that the AgoshRNA variants differ significantly in their intrinsic silencing activity.

Application of the optimized AgoshRNA triloop

To extend the current observations to other AgoshRNAs, we introduced the optimized AGA loop on 5 anti-HIV-1 AgoshRNAs (Gag5, Gag6, Pol1, Pol8 and R/T5). Silencing

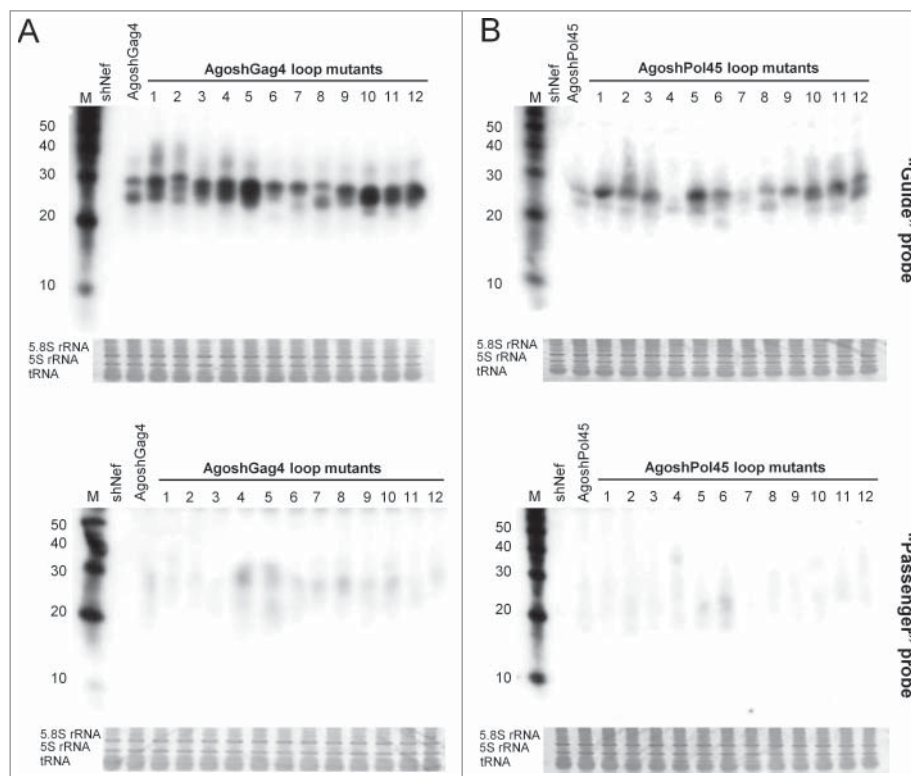


Figure 5. Northern blot analysis of the AgoshRNA processing. Processing of the AgoshGag4 (A) and AgoshPol45 (B) loop mutants was analyzed by Northern blot analysis with the "guide" probe (upper panels) and the "passenger" probe (lower panels). Ethidium bromide staining of small rRNA and tRNA are shown below the blot as loading controls.

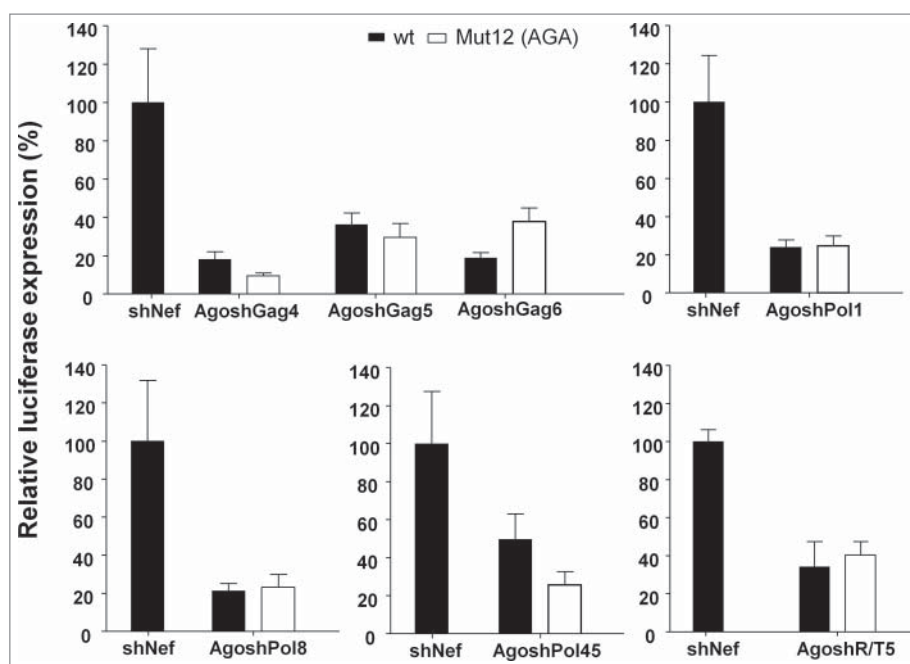


Figure 6. Effect of the novel AGA loop on other AgoshRNAs. Luciferase knockdown by AgoshRNA loop mutants was determined by co-transfection of the luciferase sense reporter for Gag5, Pol1, Pol8, Pol45 or R/T5 with 5 ng of the AgoshRNA constructs. Five separate panels are shown according to the luciferase reporter used. An irrelevant shRNA (shNef) served as negative control, for which the activity was set at 100% luciferase expression. The mean values and standard deviation are based on 6 independent transfections.

of luciferase reporters carrying the respective targets (100 ng) was measured upon co-transfection in HEK293T with the loop-substituted AgoshRNA constructs at a sub-optimal concentration (5 ng) to allow increased activity to be measured (Fig. 6). We plotted 5 separate panels as each AgoshRNA required its own luciferase reporter. The relative luciferase expression was determined by the ratio of firefly and renilla activities. Luciferase expression measured with an irrelevant shRNA (shNef) was set at 100%. The efficacy of AgoshGag4 and AgoshPol45 was 2-fold higher when the wt loop was replaced by AGA (Mut12), as described previously in Fig. 2. However, the efficacy of AgoshGag5 was only slightly increased by the AGA loop, and a wt-like knockdown activity was measured for AgoshPol1 and AgoshRT5. Even more so, insertion of the AGA loop in AgoshGag6 resulted in a 2-fold decreased activity. Thus, the tri-loop AGA does not improve the silencing activity of all AgoshRNA molecules. These combined results indicate that

the sequence identity of the loop is an important, but context-dependent determinant of AgoshRNA activity and that there may be other, yet undisclosed molecular determinants of AgoshRNA activity.

Discussion

We previously defined some parameters for the design of optimized AgoshRNA molecules: a small 5 nt loop (CAAGA) and a duplex length of 18 bp with a bottom A C mismatch, but there may be other important molecular determinants of activity. Several studies described that the loop sequence of miRNAs and shRNAs can affect the silencing activity.^{25,33,34} We now tested several loop configurations for the AgoshRNA design. We tested whether the loop identity influences AgoshRNA processing, the intracellular stability and - most importantly - silencing activity. Hairpin loops that differ in size and sequence were studied. Only small loops (3–5 nt) were used because large

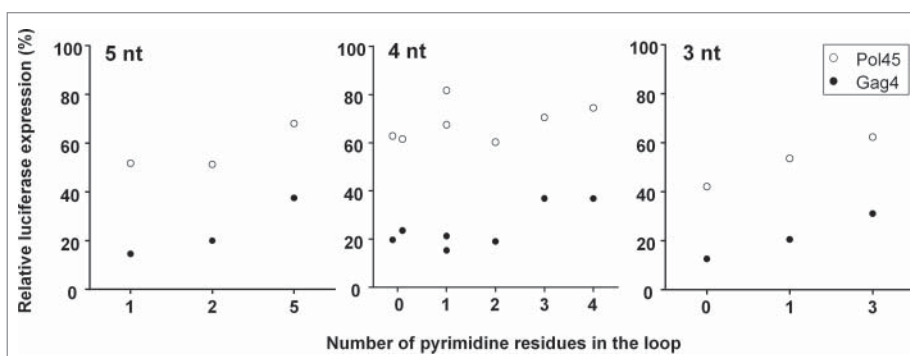


Figure 7. Influence of the loop pyrimidine content on AgoshRNA-mediated silencing. Luciferase knockdown values by AgoshGag4 (black dots) and AgoshPol45 (white dots) variants were arranged according to the number of pyrimidine residues in the loop. The data set was grouped according to the loop size.

loops (> 7 nt) cause a partial return to regular Dicer processing.²⁸ Twelve mutant loops were incorporated in 2 anti-HIV-1 AgoshRNA molecules. We document that the loop size among these small loops (3–5 nt) does not influence the RNAi activity. However, the AgoshRNA loop sequence affects its activity. Surprisingly, close inspection of the experimental data and a reanalysis for each loop size suggested that the Pu/Py composition is of importance, as illustrated in Fig. 7. We observed impaired silencing activity for AgoshRNA variants with a high Py content in the loop.

As we described previously steric hindrance for large (> 7 nt) AgoshRNA loops with the PAZ domain of Ago2, one could hypothesize that “small” Py nt should be preferred over “big” Pu nt.²⁸ However, we measured a strong preference for Pu-rich loops across different mutant sets. What could be the underlying reason for this Pu-preference? We did not observe a particular Pu-preference in natural miRNAs (results not shown). Inspection of the thermodynamic stability of the mutant set of hairpins did not reveal a correlation with the differential activity. Recently, it was suggested that Pu may facilitate RNA loading into Ago through sequence-independent interactions.³⁵ The PAZ domain of Ago proteins contains a large number of invariant aromatic residues that are involved in RNA binding and it was suggested that stacking or hydrophobic interactions of these residues with the Pu-rich miRNA strand may contribute to strand selection.^{36–38} Thus, it is conceivable that a Pu-loop may contribute to a stable interaction between the PAZ domain and the extended guide strand of AgoshRNA molecules, which will likely contribute to efficient mRNA degradation. Alternatively, one could hypothesize that the Pu-rich loop acts as binding site for a cellular co-factor that affects subsequent mRNA cleavage. Recently, the proteomic characterization of endogenous Ago2-associated RISC in red blood cells revealed several cofactor candidates, but their role remains currently unknown.³⁹

Other AgoshRNA questions were addressed. First, we extended the mRNA-complementarity of the AgoshRNA guide “over the loop,” but measured no increased knockdown potency. Second, we tried to optimize the AgoshRNA design by introduction of the miR-451 loop. This loop may facilitate Ago2-mediate processing or silencing as its sequence is evolutionary conserved, but no improved activity was scored for this mutant. Third, we introduced a loop resistant to RNA degradation (CUUG), but did not improve AgoshRNA efficacy. Only the AGA triloop seems to consistently enhance gene knockdown in reporter assays and HIV-1 inhibition assays, both for AgoshGag4 and AgoshPol45. The effect was more pronounced for the moderately active AgoshPol45, especially at low AgoshRNA concentrations. We tested the optimized AGA loop on several anti-HIV-1 AgoshRNAs, but the triloop did not improve the silencing activity of all molecules. Thus, the sequence identity of the loop is an important, but context-dependent determinant of AgoshRNA activity.

It is important to realize that existing siRNA design algorithms cannot be applied to the design of AgoshRNA molecules, which thus remains a difficult trial-and-error process.^{9,40–42} This report, in combination with previous studies, indicates that an active AgoshRNA should have a short stem-length (≤ 18 bp), a small Pu-rich loop of 3–

5 nt, and a bottom A C mismatch. Using these design rules, we plan to develop potent and non-toxic AgoshRNAs against HIV-1.

Material and methods

Plasmid construction

For the AgoshRNA constructs, DNA oligonucleotides encoding the AgoshRNA sequence with BamHI and HindIII sites were annealed and inserted into corresponding restriction sites of the pSUPER vector.⁴³ All AgoshRNA constructs were sequence-verified using the BigDye Terminator Cycle Sequencing kit (ABI). For sequencing of AgoshRNA constructs a sample denaturation temperature of 98°C was used and 1M β -actin was included in the reaction mixture. Firefly luciferase reporter constructs (pGL3; Promega) were made by insertion of a 50 to 70 nt HIV-1 sequence, with the 18 nt target region in the center, in the EcoRI and PstI sites of the pGL3 plasmid.⁴⁴ The luciferase reporter target sequences were described previously.⁴⁵

Cell culture

Human embryonic kidney 293T (HEK293T) adherent cells (ATCC CRL-11268) were grown as monolayer in Dulbecco’s modified Eagle’s medium (Life Technologies) supplemented with 10% fetal calf serum (FCS), penicillin (100 U/ml), streptomycin (100 μ g/ml) and minimal essential medium non-essential amino acids (DMEM/10% FCS) in a humidified chamber at 37°C and 5% CO₂.

DNA transfections

For luciferase assays, HEK293T cells were seeded one day before transfection in 24-wells plates at a density of 1.2×10^5 cells per well in 500 μ l DMEM/10% FCS without antibiotics. The cells were co-transfected with 100 ng firefly luciferase reporter construct and the AgoshRNA construct with Lipofectamine 2000 reagent (Invitrogen) according to the manufacturer’s instructions. To normalize for cell viability and transfection efficiency, 1 ng of pRL plasmid (Promega) expressing renilla luciferase from the CMV promoter was included. We added pBluescript SK- (pBS) (Promega) to obtain equal DNA concentrations. Two days post-transfection, firefly and renilla luciferase expression was measured in cell lysates using the Dual-Luciferase Reporter Assay System (Promega) according to the manufacturer’s instructions. Relative luciferase activities were calculated from the ratio between firefly and renilla luciferase expression. We performed 3 independent transfections, each in duplicate. Values were corrected for between-session variation as described previously.⁴⁶ The resulting 6 values were used to calculate the standard deviation shown as error bar.

For transient HIV-1 inhibition assays, HEK293T cells were seeded as described previously and co-transfected using Lipofectamine 2000 with 250 ng of the full-length HIV-1 molecular clone pLAI,⁴⁷ 1 ng of pRL-CMV and 25 ng of AgoshRNA construct. We added pBS to create an equal DNA concentration

per transfection. Two days post-transfection, virus production was determined by measuring the CA-p24 levels in the culture supernatant by ELISA.⁴⁸ Cell lysates were made to measure the renilla luciferase activity with the Renilla Luciferase Assay System (Promega) according to the manufacturer's instructions. Relative HIV-1 production was calculated as the ratio between the CA-p24 level and the renilla luciferase activity. We performed 3 independent transfections, each in duplicate. Values were corrected for between-session variation as described previously.⁴⁶

AgoshRNA detection by RNA gel blot analysis

Northern blotting was performed as described previously.¹⁴ Briefly, 1.5×10^6 HEK293T cells were transfected with 5 μ g of wt or mutant AgoshRNA construct using Lipofectamine 2000. Total cellular RNA was extracted 2 d post-transfection with the mirVana miRNA isolation kit (Life Technologies) according to the manufacturer's instructions. The RNA concentration was measured by Nanodrop 1000 (Thermo Fisher Scientific). For RNA gel blot analysis, 15 μ g total RNA was electrophoresed in a 15% denaturing polyacrylamide gel (precast Novex TBU gel, Life Technologies). The Decade RNA molecular weight marker (Life Technologies) was prepared according to the manufacturer's protocol and run alongside the cellular RNA. rRNA was stained with 2 μ g/ml ethidium bromide and visualised under UV light to ensure equal sample loading. The RNA in the gel was electro-transferred to a positively charged nylon membrane (Boehringer Mannheim GmbH) and crosslinked to the membrane using UV light at a wavelength of 254 nm (1200 μ J x 100). Overnight hybridization was performed at 42°C with radiolabeled locked nucleic acid (LNA) oligonucleotides in 10 ml ULTRAhyb hybridization buffer (Life Technologies, Austin, TX) according to the manufacturer's instructions. LNA oligonucleotide probes were 5'-end labeled with the kinaseMax kit (Life Technologies) in the presence of 1 μ l [γ -³²P] ATP (0.37 MBq/ μ l, Perkin Elmer). To remove unincorporated nt, the probes were purified on Sephadex G-25 spin columns (Amersham Biosciences) according to the manufacturer's protocol.

We used the following oligonucleotides to detect the (5') guide strand of the AgoshRNA (LNA-positions are underlined): Gag: 5'-GAAGAAATGATGACAGCAT-3', and Pol: 5'-GTGAAGGGGCAGTAGTAAT-3'. To detect the (3') passenger strand of the AgoshRNA the following oligonucleotides were used (LNA positions are underlined): Gag: 5'-ATGCTGTCATCATTTCTTC-3' and Pol: 5'-ATTACTACTGCCCTTCAC-3'. After overnight hybridization, the membranes were washed twice for 5 min at 42°C in 2 x SSC/0.1% SDS and twice for 15 min at 42°C in 0.1 x SSC/0.1% SDS. Signals were detected by autoradiography using a phosphorimager (Amersham Biosciences).

Small RNA library preparation and SOLiD deep sequencing

HEK293T cells were co-transfected with 5 μ g Ago2-FLAG plasmid and AgoshRNA-expressing plasmids. Two days post-transfection, cytoplasmic cell extracts were prepared by the treatment of cells on ice for 20 min with IsoB-NP-40 [10 mM

Tris-HCl (pH 7.9), 150 mM NaCl, 1.5 mM MgCl₂, 1% NP-40] followed by a centrifugation at 12000 g for 10 min at 4°C. The supernatant was incubated with 75 μ l of anti-FLAG M2 agarose beads (Sigma) with constant rotation overnight at 4°C. The beads were washed 3 times in NET-1 buffer [50 mM Tris-HCl (pH 7.5), 150 mM NaCl, 2.5% Tween 20]. Small RNAs associated with Ago2 were isolated by phenol chloroform extraction followed by DNase treatment using the TURBO DNA-free kit (Life Technologies). 5 μ g RNA was loaded on a denaturing 15% PAGE gel for size fractionation. The 15–55 nt RNA fragments were isolated using a Spin Column (Ambion). The quality of the RNA was assayed on a Bioanalyzer 2100 (Agilent) using a small RNA chip and served as template to create an RNA library that is compatible with the SOLiD sequencing platform. We used the SOLiD Small RNA Library Preparation protocol according to manufacturer's instructions (Applied biosystems; 4452437 Rev. B; page 51 – 66). Samples were run on a SOLiD Wildfire system (Applied biosystems).

Bioinformatics

Analysis of the SOLiD colorspace reads was performed with LifeScope Genomic Analysis Software version 2.5 (Applied biosystems) using the small RNA pipeline. First the libraries were mapped against filter-sequences to eliminate reads generated from irrelevant sources (like tRNA, adaptors sequences etc). The remaining reads are subsequently filtered against known miRNA sequences from miRBase (<http://www.mirbase.org/>) and the unmapped reads are aligned to reference sequences of AgoshRNA expressing plasmids, allowing no mismatches during alignment.

Disclosure of potential conflicts of interest

No potential conflicts of interest were disclosed.

Acknowledgment

We thank Aldo Jongejan and Antoine van Kampen for advice concerning the deep sequencing strategy.

Funding

This work was supported by the Nederlandse Organisatie voor Wetenschappelijk Onderzoek - Chemische Wetenschappen (NWO-CW, Top Grant) and Zorg Onderzoek Nederland - Medische Wetenschappen (ZonMw, Translational Gene Therapy Grant).

References

1. Bartel DP. MicroRNAs: target recognition and regulatory functions. *Cell* 2009; 136:215-33; PMID:19167326; <https://doi.org/10.1016/j.cell.2009.01.002>
2. Brummelkamp TR, Bernards R, Agami R. A system for stable expression of short interfering RNAs in mammalian cells. *Science* 2002; 296:550-3; PMID:11910072; <https://doi.org/10.1126/science.1068999>
3. Carthew RW, Sontheimer EJ. Origins and mechanisms of miRNAs and siRNAs. *Cell* 2009; 136:642-55; PMID:19239886; <https://doi.org/10.1016/j.cell.2009.01.035>

4. Berkhout B. Toward a durable anti-HIV gene therapy based on RNA interference. *Ann N Y Acad Sci* 2009; 1175:3-14; PMID:19796072; <https://doi.org/10.1111/j.1749-6632.2009.04972.x>
5. Chendrimada TP, Gregory RI, Kumaraswamy E, Norman J, Cooch N, Nishikura K, Shiekhattar R. TRBP recruits the Dicer complex to Ago2 for microRNA processing and gene silencing. *Nature* 2005; 436:740-4; PMID:15973356; <https://doi.org/10.1038/nature03868>
6. Jaskiewicz L, Filipowicz W. Role of Dicer in posttranscriptional RNA silencing. *Curr Top Microbiol Immunol* 2008; 320:77-97; PMID:18268840; https://doi.org/10.1007/978-3-540-75157-1_4
7. Siomi H, Siomi MC. Posttranscriptional regulation of microRNA biogenesis in animals. *Mol Cell* 2010; 38:323-32; PMID:20471939; <https://doi.org/10.1016/j.molcel.2010.03.013>
8. Khvorova A, Reynolds A, Jayasena SD. Functional siRNAs and miRNAs exhibit strand bias. *Cell* 2003; 115:209-16; PMID:14567918; [https://doi.org/10.1016/S0092-8674\(03\)00801-8](https://doi.org/10.1016/S0092-8674(03)00801-8) 10.1016/S0092-8674(03)00893-6
9. Schwarz DS, Hutvagner G, Du T, Xu Z, Aronin N, Zamore PD. Asymmetry in the assembly of the RNAi enzyme complex. *Cell* 2003; 115:199-208; PMID:14567917; [https://doi.org/10.1016/S0092-8674\(03\)00759-1](https://doi.org/10.1016/S0092-8674(03)00759-1)
10. Yang JS, Maurin T, Robine N, Rasmussen KD, Jeffrey KL, Chandwani R, Papapetrou EP, Sadelain M, O'Carroll D, Lai EC. Conserved vertebrate mir-451 provides a platform for Dicer-independent, Ago2-mediated microRNA biogenesis. *Proc Natl Acad Sci U S A* 2010; 107:15163-8; PMID:20699384; <https://doi.org/10.1073/pnas.1006432107>
11. Cifuentes D, Xue H, Taylor DW, Patnode H, Mishima Y, Cheloufi S, Ma E, Mane S, Hannon GJ, Lawson ND, et al. A novel miRNA processing pathway independent of Dicer requires Argonaute2 catalytic activity. *Science* 2010; 328:1694-8; PMID:20448148; <https://doi.org/10.1126/science.1190809>
12. Cheloufi S, Dos Santos CO, Chong MM, Hannon GJ. A dicer-independent miRNA biogenesis pathway that requires Ago catalysis. *Nature* 2010; 465:584-9; PMID:20424607; <https://doi.org/10.1038/nature09092>
13. Yoda M, Cifuentes D, Izumi N, Sakaguchi Y, Suzuki T, Giraldez AJ, Tomari Y. Poly(A)-specific ribonuclease mediates 3'-end trimming of Argonaute2-cleaved precursor microRNAs. *Cell Rep* 2013; 5:715-26; PMID:24209750; <https://doi.org/10.1016/j.celrep.2013.09.029>
14. Herrera-Carrillo E, Harwig A, Liu YP, Berkhout B. Probing the shRNA characteristics that hinder Dicer recognition and consequently allow Ago-mediated processing and AgoshRNA activity. *RNA* 2014; 20:1410-8; PMID:25035295; <https://doi.org/10.1261/rna.043950.113>
15. Herrera-Carrillo E, Harwig A, Berkhout B. Toward optimization of AgoshRNA molecules that use a non-canonical RNAi pathway: variations in the top and bottom base pairs. *RNA Biol* 2015; 12:447-56; PMID:25747107; <https://doi.org/10.1080/15476286.2015.1022024>
16. Harwig A, Herrera-Carrillo E, Jongejan A, van Kampen AH, Berkhout B. Deep sequence analysis of AgoshRNA processing reveals 3' A addition and trimming. *Mol Ther Nucleic Acids* 2015; 4:e247; PMID:26172504; <https://doi.org/10.1038/mtna.2015.19>
17. Liu YP, Schopman NC, Berkhout B. Dicer-independent processing of short hairpin RNAs. *Nucleic Acids Res* 2013; 41:3723-33; PMID:23376931; <https://doi.org/10.1093/nar/gkt036>
18. Dallas A, Ilves H, Ge Q, Kumar P, Shorestein J, Kazakov SA, Cuellar TL, McManus MT, Behlke MA, Johnston BH. Right- and left-loop short shRNAs have distinct and unusual mechanisms of gene silencing. *Nucleic Acids Res* 2012; 40:9255-71; PMID:22810205; <https://doi.org/10.1093/nar/gks662>
19. Bridge AJ, Pebernard S, Ducraux A, Nicoloulz AL, Iggo R. Induction of an interferon response by RNAi vectors in mammalian cells. *Nat Genet* 2003; 34:263-4; PMID:12796781; <https://doi.org/10.1038/ng1173>
20. Berkhout B, Liu YP. Towards improved shRNA and miRNA reagents as inhibitors of HIV-1 replication. *Future Microbiol* 2014; 9:561-71; PMID:24810353; <https://doi.org/10.2217/fmb.14.5>
21. Liu YP, Karg M, Herrera-Carrillo E, Berkhout B. Towards antiviral shRNAs based on the AgoshRNA design. *PLoS One* 2015; 10:e0128618; PMID:26087209; <https://doi.org/10.1371/journal.pone.0128618>
22. Herrera-Carrillo E, Gao ZL, Harwig A, Heemskerk MT, Berkhout B. The influence of the 5-terminal nucleotide on AgoshRNA activity and biogenesis: importance of the polymerase III transcription initiation site. *Nucleic Acids Res* 2017; 45:4036-50; PMID:27928054; <https://doi.org/10.1093/nar/gkw1203>
23. Frank F, Sonenberg N, Nagar B. Structural basis for 5'-nucleotide base-specific recognition of guide RNA by human AGO2. *Nature* 2010; 465:818-22; PMID:20505670; <https://doi.org/10.1038/nature09039>
24. Hu HY, Yan Z, Xu Y, Hu H, Menzel C, Zhou YH, Chen W, Khaitovich P. Sequence features associated with microRNA strand selection in humans and flies. *BMC Genomics* 2009; 10:413; PMID:19732433; <https://doi.org/10.1186/1471-2164-10-413>
25. Hinton TM, Wise TG, Cottee PA, Doran TJ. Native microRNA loop sequences can improve short hairpin RNA processing for virus gene silencing in animal cells. *J RNAi Gene Silencing* 2008; 4:295-301; PMID:19771239
26. Liu G, Min H, Yue S, Chen CZ. Pre-miRNA loop nucleotides control the distinct activities of mir-181a-1 and mir-181c in early T cell development. *PLoS One* 2008; 3:e3592; PMID:18974849; <https://doi.org/10.1371/journal.pone.0003592>
27. Michlewski G, Guil S, Semple CA, Caceres JF. Posttranscriptional regulation of miRNAs harboring conserved terminal loops. *Mol Cell* 2008; 32:383-93; PMID:18995836; <https://doi.org/10.1016/j.molcel.2008.10.013>
28. Wang Y, Juranek S, Li H, Sheng G, Tuschl T, Patel DJ. Structure of an argonaute silencing complex with a seed-containing guide DNA and target RNA duplex. *Nature* 2008; 456:921-6; PMID:19092929; <https://doi.org/10.1038/nature07666> 10.1038/454921e 10.1038/nature07315
29. Lai EC. microRNAs: runts of the genome assert themselves. *Curr Biol* 2003; 13:R925-36; PMID:14654021; <https://doi.org/10.1016/j.cub.2003.11.017>
30. Jucker FM, Pardi A. Solution structure of the CUUG hairpin loop: a novel RNA tetraloop motif. *Biochemistry* 1995; 34:14416-27; PMID:7578046; <https://doi.org/10.1021/bi00044a019>
31. Sun G, Yeh SY, Yuan CW, Chiu MJ, Yung BS, Yen Y. Molecular properties, functional mechanisms, and applications of sliced siRNA. *Mol Ther Nucleic Acids* 2015; 4:e221; PMID:25602583; <https://doi.org/10.1038/mtna.2014.73>
32. Ge Q, Ilves H, Dallas A, Kumar P, Shorestein J, Kazakov SA, Johnston BH. Minimal-length short hairpin RNAs: the relationship of structure and RNAi activity. *RNA* 2010; 16:106-17; PMID:19952116; <https://doi.org/10.1261/rna.1894510>
33. Schopman NC, Liu YP, Konstantinova P, Ter Brake O, Berkhout B. Optimization of shRNA inhibitors by variation of the terminal loop sequence. *Antiviral Res* 2010; 86:204-11; PMID:20188764; <https://doi.org/10.1016/j.antiviral.2010.02.320>
34. McManus MT, Petersen CP, Haines BB, Chen J, Sharp PA. Gene silencing using micro-RNA designed hairpins. *RNA* 2002; 8:842-50; PMID:12088155; <https://doi.org/10.1017/S1355838202024032>
35. Hu HY, Yan Z, Xu Y, Hu H, Menzel C, Zhou YH, Chen W, Khaitovich P. Sequence features associated with microRNA strand selection in humans and flies. *BMC Genomics* 2009; 10:413; PMID:19732433; <https://doi.org/10.1186/1471-2164-10-413>
36. Preall JB, Sontheimer EJ. RNAi: RISC gets loaded. *Cell* 2005; 123:543-5; PMID:16286001; <https://doi.org/10.1016/j.cell.2005.11.006>
37. Song JJ, Smith SK, Hannon GJ, Joshua-Tor L. Crystal structure of Argonaute and its implications for RISC slicer activity. *Science* 2004; 305:1434-7; PMID:15284453; <https://doi.org/10.1126/science.1102514>
38. Ming D, Wall ME, Sanbonmatsu KY. Domain motions of Argonaute, the catalytic engine of RNA interference. *BMC Bioinformatics* 2007; 8:470; PMID:18053142; <https://doi.org/10.1186/1471-2105-8-470>
39. Azzouzi I, Moest H, Wollscheid B, Schmutz M, Eekels JJ, Speer O. Deep sequencing and proteomic analysis of the microRNA-induced silencing complex in human red blood cells. *Exp Hematol* 2015; 43:382-92; PMID:25681748; <https://doi.org/10.1016/j.exphem.2015.01.007>
40. Khvorova A, Reynolds A, Jayasena SD. Functional siRNAs and miRNAs exhibit strand bias. *Cell* 2003; 115:209-16; PMID:14567918; [https://doi.org/10.1016/S0092-8674\(03\)00801-8](https://doi.org/10.1016/S0092-8674(03)00801-8) 10.1016/S0092-8674(03)00893-6
41. Reynolds A, Leake D, Boese Q, Scaringe S, Marshall WS, Khvorova A. Rational siRNA design for RNA interference. *Nat Biotechnol* 2004; 22:326-30; PMID:14758366; <https://doi.org/10.1038/nbt936>
42. Tomari Y, Zamore PD. Perspective: machines for RNAi. *Genes Dev* 2005; 19:517-29; PMID:15741316; <https://doi.org/10.1101/gad.1284105>

43. Fire A, Xu S, Montgomery MK, Kostas SA, Driver SE, Mello CC. Potent and specific genetic interference by double-stranded RNA in *Caenorhabditis elegans*. *Nature* 1998; 391:806-11; PMID:9486653; <https://doi.org/10.1038/35888>
44. Westerhout EM, Ooms M, Vink M, Das AT, Berkhout B. HIV-1 can escape from RNA interference by evolving an alternative structure in its RNA genome. *Nucleic Acids Res* 2005; 33:796-804; PMID:15687388; <https://doi.org/10.1093/nar/gki220>
45. Ter Brake O, Konstantinova P, Ceylan M, Berkhout B. Silencing of HIV-1 with RNA interference: a multiple shRNA approach. *Mol Ther* 2006; 14:883-92; PMID:16959541; <https://doi.org/10.1016/j.ymthe.2006.07.007>
46. Ruijter JM, Thygesen HH, Schoneveld OJ, Das AT, Berkhout B, Lamers WH. Factor correction as a tool to eliminate between-session variation in replicate experiments: application to molecular biology and retrovirology. *Retrovirology* 2006; 3:2; PMID:16398936; <https://doi.org/10.1186/1742-4690-3-2> 10.1186/1742-4690-3-S1-S2 10.1186/1742-4690-3-S1-P2
47. Peden K, Emerman M, Montagnier L. Changes in growth properties on passage in tissue culture of viruses derived from infectious molecular clones of HIV-1_{LAI}, HIV-1_{MAL}, and HIV-1_{ELL}. *Virology* 1991; 185:661-72; PMID:1683726; [https://doi.org/10.1016/0042-6822\(91\)90537-L](https://doi.org/10.1016/0042-6822(91)90537-L)
48. Jeeninga RE, Hoogenkamp M, Armand-Ugon M, de Baar M, Verhoef K, Berkhout B. Functional differences between the long terminal repeat transcriptional promoters of human immunodeficiency virus type 1 subtypes A through G. *J Virol* 2000; 74:3740-51; PMID:10729149; <https://doi.org/10.1128/JVI.74.8.3740-3751.2000>
49. Herrera-Carrillo E, Harwig A, Berkhout B. Silencing of HIV-1 by AgoshRNA molecules. *Gene Ther.* 2017 May 29; PMID: 28553929; <https://doi.org/10.1038/gt.2017.44>